Well Trap Structures and Bulk-nano Environment Luminescence Centers in $CaZnGe_2O_6:Tb^{3+}$ Long Afterglow Phosphor

Boon Kuan Woo[1], Yang Li[2], Surinder P. Singh[2]

[1]Department of Physics, University of Texas at Arlington, Arlington, TX 76019-0059, Faculty of Engineering, Multimedia University, Cyberjaya campus, Selangor, Malaysia, bkwoo@mmu.edu.my
[2] Department of Engineering Science and Materials, University of Puerto Rico, Mayaguez, PR 00680, USA

ABSTRACT

A long afterglow phosphor $CaZnGe_2O_6:Tb^{3+}$ has been prepared by using organic coated luminescence ZnO nanopowder through a high temperature solid-state reaction route. This new $CaZnGe_2O_6:Tb^{3+}$ long afterglow phosphor sample emits the Tb^{3+} green fluorescence 543 nm emission corresponding to $^5D_4 \rightarrow {}^7F_5$ transition under UVA 350 nm illumination. The organic coated luminescence ZnO nanopowder serves to construct shallow well trap for the Tb^{3+} dopant and to minimize electron leakage of well traps. By adjusting the mass ratio of both the bulk ZnO powder (<1000 nm size) and the organic coated luminescence ZnO nanopowder (5-10 nm size), depth of well traps that dictate luminescence and afterglow properties could be controlled. The optimized long afterglow phosphor sample was found to be made of 70% gm-weight of bulk ZnO powder and 50% gm-weight of organic coated luminescence ZnO nanopowder or $CaZn_{0.83}Ge_2O_6:Tb^{3+}$ phase compound that exhibit afterglow longevity of longer than 3 hours. Therefore, phosphorescence effect is best explained based upon well trap structures model and structure lattice defects play an important role in influencing persistent luminescence phenomena.

Keywords: persistent luminescence, photoluminescence, long afterglow phosphor, ZnO nanoparticles, rare earth dopants

1 INTRODUCTION

In the past decade, research on afterglow phosphor materials that has long decay lifetime has attracted the attention of many researchers. Afterglow phosphor materials have their potential applications in display technology as well as in detection of high energy radiation beams such as X-ray, cathode-ray, UV ray and beta ray. Among the many afterglow phosphor materials, so far the rare-earth ions doped alkali earth aluminates and oxysulfide based phosphors have been aggressively explored and utilized broadly. Theoretically, long lasting afterglow phosphor is believed due to thermally stimulated recombination of electrons and holes stored in the traps at room temperature and the afterglow properties depend on the trap density, trap depth and host lattice. However, the exact nature of the trap and the mechanism of capturing and releasing the light energy remain largely unknown, therefore it is in our interest that by making use of our organic coated luminescence ZnO nanopowder in phosphor preparations, we hope to gain a deep and clear understandings behind the afterglow mechanisms, even though our original goal was to utilize them for biomedical applications. We devoted our attention to alkali earth germinates based phosphors with Tb^{3+} doping as the main activator.

In this paper, we prepared our afterglow phosphor samples by using both the bulk ZnO powder and organic coated luminescence ZnO nanopowder, prepared via wet chemistry route [1] as precursor through high temperature solid-state reaction.

2 EXPERIMENTS

The afterglow phosphor powder samples were prepared according to stoichiometric proportions with the following amounts of Germanium (IV) oxide [0.878 gm, 8.4 mmole, 99.998%], Calcium (II) oxide [0.235 gm, 4.2 mmole, 99.9%], Bulk Zinc oxide powder and/or organic coated luminescence ZnO nanopowder [Total mass of 0.342 gm, 4.2 mmole or 100% gm-weight, 99.9% for bulk] and Terbium (III, IV) oxide [0.03 gm, 0.04 mmole, 99.999%, 3.8 mol% Tb^{3+}]. All chemicals were obtained and purchased from Sigma-Aldrich with the exception of the organic coated luminescence ZnO nanopowder. All powders were thoroughly mixed together, placed in a covered alumina crucible, pre-heated at 200℃ for 1 hour and finally annealed at 1100℃ for 1 hour under normal atmospheric condition. Approximately 1.3 gm of hardened white sample in shallow bowl chunk shape was obtained.

3 RESULTS AND DISCUSSION

Figure 1(a) shows a TEM image of a grain particle of the afterglow sample made from 100% gm-weight organic

coated luminescence ZnO nanopowder. From the magnified high-resolution TEM (HRTEM) images in (b-d), it is estimated that the near squared lattice spacing in the particle to be 1 nm which corresponds to (100) and (010) planes, respectively, along the [001] zone axis. Figure 1(e) is the electron diffraction pattern of the [001] zone axis, where the reflection conditions are: $h = 2n$ for $h00$, and $k = 2n$ for $0k0$, where n is an integer. Some visible reflections at the forbidden sites are formed by double reflections. The reflection conditions are consistent to its space group $C2/c$. The EDS data in Figure 1(f) clearly indicates that terbium atoms have been successfully doped into $CaZnGe_2O_6$ host lattice and with no traces of carbon impurities.

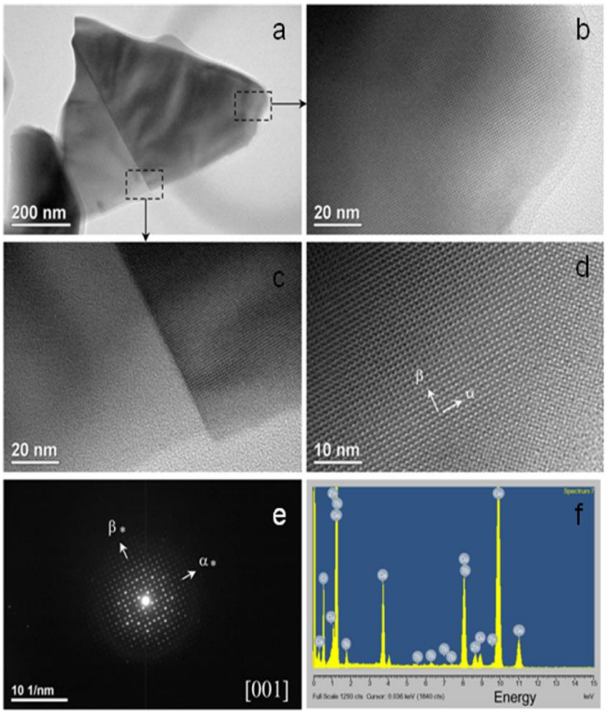

Figure 1. TEM/EDS data on $CaZnGe_2O_6:Tb^{3+}$ afterglow phosphor made of 100% gm-weight organic coated luminescence ZnO nanopowder.

The best possible mechanism to explain long lasting afterglow is based upon the nature of well traps [2-9]. Samples with shallow well traps tend to give short burst of afterglow while samples with very deep well traps may not give phosphorescence at all at room temperature. The best approach is to fabricate samples with middle-size depth well traps by combining both the shallow well traps and deep well traps. However, this is only possible if we could identify the key elements that could construct physical well trap structure within the host lattice material. In our study of $CaZnGe_2O_6:Tb^{3+}$ phosphorescence material, we found that the crucial well-building material is zinc oxide. First, 3 samples were made with 100% gm-weight from bulk ZnO powder, commercially available ZnO nanopowder and organic coated luminescence ZnO nanopowder. Their physical and optical properties were observed and compared. We observe that samples made from bulk ZnO powder and ZnO nanopowder exhibited same physical appearances and optical properties while the sample made from the organic coated luminescence ZnO nanopowder gives us different optical properties, not yet reported before. Figure 2 shows us the optical properties of $CaZnGe_2O_6:Tb^{3+}$ made of 100% gm-weight organic coated luminescence ZnO nanopowder as compared to sample made of 100% gm-weight bulk ZnO. This new emerging seven excitation peaks (303 nm, 317 nm, 339 nm, 353 nm, 369 nm, 379 nm and 486 nm corresponding to $^7F_6$-$^3H_6$, $^7F_6$-$^5D_0$, $^7F_6$-$^5L_7$, $^7F_6$-$^5L_9$, $^7F_6$-$^5G_5$, $^7F_6$-$^5G_6$ and $^7F_6$-$^5D_4$ transitions of Tb^{3+}, respectively) has us convinced that the organic coated luminescence ZnO nanoparticles are responsible for constructing the shallow well traps in this afterglow phosphor material. Beside revealing the 4f to 5d transitions, the excitation spectra also revealed that the Tb^{3+} dopants are surrounded by host lattice environment that enable the electrons to be easily excited by less energetic photons. The broad absorption band centers around 265 nm is believed due to host absorption band in which energy transfer could occur from host lattice phosphor onto the dopant species.

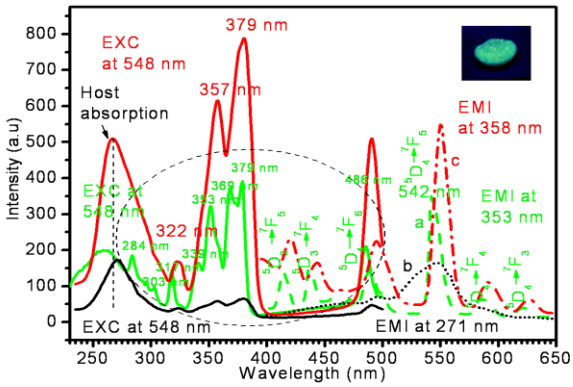

Figure 2. Optical properties of three $CaZnGe_2O_6:Tb^{3+}$ afterglow phosphors a) 100% gm-weight organic coated luminescence ZnO nanopowder (green), b) 100% gm-weight bulk ZnO powder (black) and c) optimized sample with 70% gm-weight bulk ZnO and 50% gm-weight nano ZnO (red).
(Inset) Optimized Tb^{3+}doped sample made of 70% gm-weight bulk ZnO and 50% gm-weight nano ZnO under UVA 350 nm illumination.

Figure 3 shows the various well trap models for this $CaZnGe_2O_6:Tb^{3+}$ long afterglow phosphor material. Once we have identified the material ingredients responsible for deep well traps (bulk ZnO) and shallow well traps (nano ZnO), we decided to fabricate hybrid afterglow phosphors to pursue our investigations. These are afterglow phosphor samples consist of mixture of bulk ZnO and organic coated luminescence ZnO nanopowder. However, before doing so, we need to establish accurately the actual mass of ZnO nanoparticles that are organic-coated. A simple heat

treatment experiment is conducted and we established that the actual ZnO nanoparticles' mass is 25.4% of the total gm-weight of the organic coated luminescence ZnO nanopowder. In order to prove that this percentage number is right, we fabricated a sample made of 70% gm-weight bulk ZnO and 118% gm-weight of organic coated luminescence ZnO nanopowder. This sample turned out as a well-crystallized solid chunk form, permanently fused onto the alumina crucible and has very high hardness, a common property found in metal alloy. This observation verified that the percentage is accurate since the calculation reveal that it fulfilled exactly the total stoichiometric mass for ZnO (0.342 gm from both bulk and nano ZnO), leaving no room for native internal defects to be formed that could weaken the physical property of the sample. Therefore, at this point, we offer this explanation that if the starting materials consist of mass deficiency in zinc oxide, air chamber enclosure tends to form onto other host lattice layer thus creating structural lattice defect.

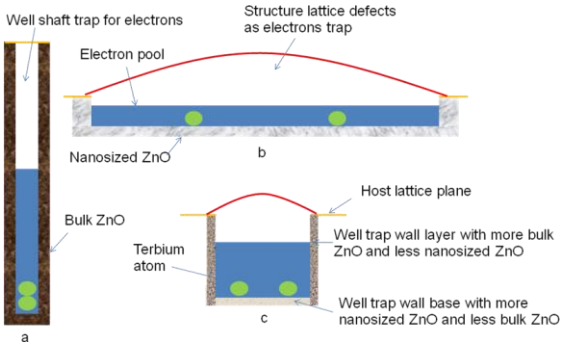

Figure 3. Various well trap structure models based on experimental samples, a) Deep well trap or " Thermos-flask", 100% gm-weight bulk ZnO b) Shallow well trap or "Frying pan", 100% gm-weight organic coated luminescence ZnO nanopowder c) Middle-depth well trap or "Hot pot", the optimized sample with 70% gm-weight bulk ZnO and 50% gm-weight organic coated luminescence ZnO

As the search continues for the hypothetical middle-depth well trap structure phosphor that could give us the best of both photoluminescence and long afterglow duration and with the high temperature furnace pushing at its limit at 1100℃, with no slurry solvent, no ball-milling, no flux material being employed and no high pressure compaction, the organic coated luminescence ZnO nanopowder prevailed and the final optimized afterglow phosphor sample, was found to be 70% gm-weight bulk ZnO and 50% gm-weight organic coated luminescence ZnO nanopowder. This sample has very good afterglow properties for both UVA 350 nm and UV 254 nm illuminations and it also fluorescence a bright green Tb^{3+}, 543 nm luminescence upon UVA 350 nm illumination. In order to explain this sample, we calculated the total mass of ZnO required in constructing its well traps to be 0.2828 gm, which is short of the proper stoichiometric value of 0.342 gm. From this information, we could deduce that the missing ZnO's mass (17.3%) is responsible for creating the inter-layer structure defect which serves as electrons trap for the photo-excited electrons.

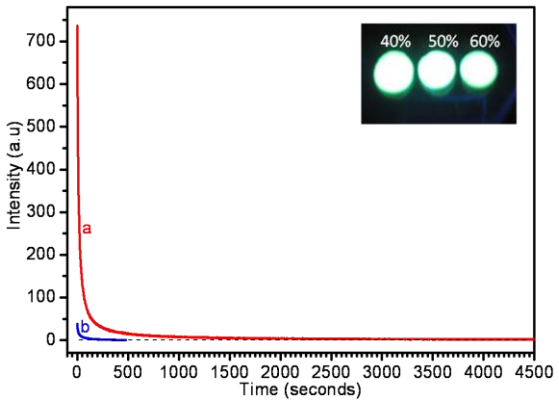

Figure 4. Comparison of afterglow decay curve lifetimes after 4 minutes exposure under UV 254 nm for a) Optimized Tb^{3+}-doped sample (70% bulk ZnO - 50% nano ZnO) and b) Tb^{3+}-doped sample made from 100% gm-weight bulk ZnO.
(Inset) Optimized Tb^{3+} doped samples made from 70% gm-weight bulk ZnO with 40%, 50%, 60% gm-weight nano ZnO under UV 254 nm illumination.

A proper observation experiment was conducted, in which we found out that the persistence luminescence (Figure 4) for the optimized sample can extend over 3 hours period with only 4 minutes exposure time of UV 254 nm.

$CaZnGe_2O_6$ is a well-known self-activated phosphor [10] and by referring to Figure 5, a comparison of optical properties of all the three undoped studied samples, we could see that there is a spectral shift of the green emission 531 nm (bulk ZnO) to 452 nm and 444 nm (luminescence nanosized ZnO). Moreover, the figure clearly shown that the undoped optimized sample (70% gm-weight bulk ZnO and 50% gm-weight nanosized ZnO) has the best capacity to contain more highly energetic hot electrons within its internal lattice structure since its blue 444 nm intensity matched the green 531 nm intensity of the sample made of 100% gm-weight bulk ZnO material.

We also believed that the blue 452 nm intensity is lower as compared to the other peaks is due to the presence of more ZnO nanoparticles in constructing the shallow well traps which has the poorest ability in containing highly energetic photo-excited electrons, a possibility in which some of these photo-excited electrons could escape via non-radiative centers. The presence of the small 354 nm excitation peaks as exhibited by samples made with organic coated luminescence ZnO nanopowder corresponded well to the notion that the ZnO nanoparticles are well integrated within the host material since we detected this same excitation peak when we measured the optical properties of

the organic coated luminescence ZnO nanopowder. These nanosized ZnO particles could also be responsible for the emergence of the blue (444 nm and 452 nm) emission centers. A more detailed XRD analysis on these new bulk-nano $CaZnGe_2O_6:Tb^{3+}$ phosphor samples have been discussed and explained in other journal publication [11, see Figure 3 and Table 2], in which the final optimized phosphor sample (70%-50% ZnO) was found to be in $CaZnGe_2O_6$ phase with 91.25 content (wt %).

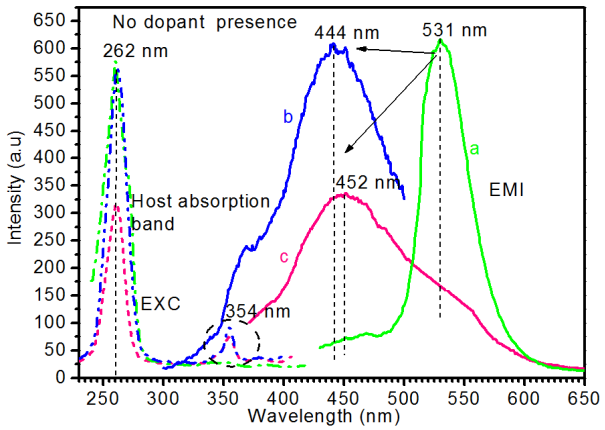

Figure 5. Optical properties comparison between a) undoped sample made of 100% gm-weight bulk ZnO powder (green) b) undoped optimized sample made of 70%-50% gm-weight bulk and nano ZnO (blue) and c) undoped sample of 100% gm-weight nano ZnO (pink).

4 CONCLUSION

In summary, phosphorescence effect of $CaZnGe_2O_6:Tb^{3+}$ long afterglow phosphor has been optimized by using bulk and nanosized ZnO material. The optimized sample has the constitution of 70% gram-weight bulk ZnO and 50% gram-weight organic coated luminescence ZnO nanopowder or $CaZn_{0.83}Ge_2O_6:Tb^{3+}$ phase compound, a middle-depth well trap structure.

Based on our experimental findings, we proposed our afterglow well trap structures model to explain persistence luminescence. There are two crucial traps in our models. The first, being the structural well trap that contains the dopant cations and the electron pool. The second, being the air chamber enclosure or structure lattice defects that serves to trap photo-excited electrons. Deep well trap has narrow well shaft trap for electrons that contributes to phosphorescence while shallow well trap has a wide surface area that is enclosed by structure lattice defects boundary which contributes to photoluminescence. By adjusting the balance of bulk-nano composition of ZnO material, the construction of the middle-depth well trap structure within the host lattice $CaZnGe_2O_6$ phosphor is thus possible. Due to the presence of ZnO nanoparticles within the well traps' bases and walls, the bulk-nano environment they created, contributed in constraining space therefore imposed a strong crystal ligand field within the host lattice material that blue-shifted the host phosphor's green emission. Works are still underway to investigate and to probe deeply the co-dopant issues involving the rare-earth (Sm^{3+}, Eu^{3+}, Dy^{3+}, Tm^{3+}, Pr^{3+}, Nd^{3+}, Yb^{3+} , Ho^{3+}, Lu^{3+} etc) and transition metal (Mn^{2+}, Cr^{3+}, Sb^{3+}, Bi^{3+}, Mg^{2+}, Na^{+}, In^{3+}, Ga^{3+}, Ti^{4+}, etc) cations by using our optimized middle-depth well trap model on this $CaZnGe_2O_6$ afterglow phosphor material. Finally, this new $CaZnGe_2O_6:Tb^{3+}$ long afterglow phosphor has excellent potential to serve as X-ray phosphor by simply tailoring its well traps' depth, active crystal medium for solid-state lasers, highly efficient phosphor for light extraction, tri-dopants approach in obtaining long lasting red afterglow and also with the possibility of advancing triboluminescence field of study.

Acknowledgements: The authors gratefully thank Dr. Marius Hossu for help in X-ray photoluminescence measurements. Special thanks to Ken and Gail Spontelli from Mansfield, Texas for proof-reading this research manuscript.

REFERENCES

1. Boon Kuan Woo, Wei Chen, Alan G. Joly, R. Sammynaiken, Journal of Physical Chemistry C (2008), 112, 14292-14296.
2. T. Matsuzawa, Y. Aoki, N. Takeuchi, Y. Murayama J. Electrochem. Soc. 143 (1996) 2670.
3. S. W. S. McKeever, in Thermoluminescence of Solids, R. W. Cahn, E. A. Davis and I. M. Ward, Editors, Cambridge University Press, Cambridge, England 1985.
4. S. Basun, G. F. Imbusch, D. Jia, and W. M. Yen, Journal of Luminescence, 104, 283, (2003).
5. Weiyi Jia, Huabiao Yuan, Lizhu Lu, Huimin Liu, William M. Yen, Journal of Crystal Growth 200 (1999) 179-184.
6. D. Jia and W. M. Yen, Journal of Luminescence, 101, 115, (2003).
7. A. A. Setlur, A. M. Srivastava, H. L. Pham, M. E. Hannah, U. Happek, Journal of Applied Physics 103 053513 (2008).
8. Dongdong Jia, Weiyi Jia, Yi Jia, Journal of Applied Physics 101, 023520 (2007).
9. T. Aitasalo, D. Hreniak, J. Holsa, T. Laamanen, M. Lastusaari, J. Nittykoski, F. Pelle, W. Strek, Journal of Luminescence, 122-123 (2007) 110-112.
10. Guangbo Che, Chunbo Liu, Xiuying Li, Zhanlin Xu, Yang Liu, Hang Wang, Journal of Physics and Chemistry of Solids, 69 (2008), 2091-2095.
11. Boon Kuan Woo, Zhiping Luo, Yang Li, Surinder P. Singh, Alan G. Joly, Marius Hossu, Zhongxin Liu, Wei Chen, Optical Materials, 33 (2011), 1283-1290.